Scanning Microscopy Vol. 12, No. 1, 1998 (Pages 31-41)
Scanning Microscopy International, Chicago (AMF O'Hare), IL 60666 USA
0891-7035/98$5.00+.25

THE EVOLUTION OF ROTATING SILICON SURFACES DURING ION BOMBARDMENT

Graham R. Carlow*

Department of Physics, The University of Western Ontario, London, Ontario, Canada, N6A 3K7

(Received for publication May 23, 1996 and in revised form November 6, 1996)

Abstract

Under a wide range of conditions, ion bombardment of nominally flat substrates results in the formation of macroscopic hummock features. We present a theoretical model of this process which details the evolution of hummocks on rotating substrates. The formation of facetted hummocks, the interaction and coalescence of two hummocks, and global properties such as the hummock size distribution are described. These results are used to interpret experimentally observed hummocks on Ar^+ sputtered, rotating Si(100) substrates.

Key words: Sputtering, silicon, hummocks, facetting, coalescence.

*Address for correspondence:
Graham R. Carlow
Department of Physics and Astronomy
The University of Western Ontario
London, Ontario, Canada N6A 3K7
Telephone number: (519) 661-3986
FAX number: (519) 661-2033
E-mail: gcarlow@julian.uwo.ca

Introduction

Ion beam modification of surfaces has received a great deal of theoretical and experimental study for more than two decades [2, 3, 5, 12, 13, 14]. Much of this interest has been stimulated by applications, such as reactive ion beam etching, secondary ion mass spectroscopy (SIMS), and ion beam thinning for transmission electron microscopy (TEM) sample preparation. For such applications, maintaining a planar surface during sputtering is of prime importance. Any surface roughness created during the sputtering process could obscure morphological features of interest in TEM, or could result in modified elemental depth profiles in SIMS or sputter/Auger techniques. However, under a wide range of conditions during the sputtering process a nominally flat surface evolves into a surface with hummock-like features.

While for most practical applications of sputtering avoidance of hummock formation is sought, recently it has been proposed that hummocks could be applied constructively to provide a means of improving the quality of strained heteroepitaxial layers [8]. For hetero-epitaxial overgrowth on a rough or patterned surface, the strain associated with the lattice mismatch of the film/substrate can be localized near the interface and the remainder of the film grows strain free [9]. However, to obtain high quality overlayers for eg., the Ge/Si system which has a 4% lattice mismatch, substrate patterning on length-scales of 20 nm or less is needed. This is an order of magnitude below the limit of photolitho-graphic techniques so at present alternate patterning techniques are necessary. Hummock formation by ion beam bombardment is one possible candidate as access to smaller length-scales can be achieved. For such constructive applications, a detailed knowledge of properties such as the hummock size distribution and hummock areal densities as well as the local properties, such as the shape of individual hummocks is required.

Previous descriptions of hummock formation and evolution from a nominally flat starting surface include continuum models of the surface [2] coupled with wavefront propagation instabilities and models which concentrate on sputtering of specific surface features [5, 12]. One common parameter in all the models is the angular dependence of the sputtering yield. A schematic plot of the sputtering yield, S, versus the angle of the ion beam with respect to the surface

normal, ϕ, is shown in Figure 1. This curve is obtained from the experimental observations of Ar^+ irradiated silicon [1, 7, 10, 11] and is a result of the (i) the energy loss of ions as they penetrate the substrate, and (ii) direct reflections of the impinging ions from the substrate [12, 14]. At small angles, reflections are rare and the details of energy loss give the increase in yield with angle, while at large angles reflections of ions from the substrate dominate and the sputtering yield is reduced. These two processes produce the curve shown which is common to most materials.

Hummock formation is typically dependent on the yield curve since microscopic features on the surface will tend to etch at different rates compared to the flat surface and, through differential etching, the initial features are enhanced and macroscopic hummocks form. Indeed, the formation of hummocks requires a microscopically rough surface since otherwise hummock formation is suppressed [5]. More specifically however, the evolution of a surface depends on the angle of the ion beam, ϕ. For example, for ϕ= 75°-85° the starting surface will in general smooth out and no hummocks form. In angular ranges of 0°-75°, hummocks tend to form, most prominently near the maximum S (ϕ≈65°). In addition to the yield curve, hummock details depend on other parameters such as the ion beam energy and the total ion dose [5]. General trends include an increase in the spatial density of hummocks with an increase in ion dose while the size of hummocks tends to increase with ion beam energy.

While no theories exist for hummock size distributions evolving during sputtering, the two main late stage cluster growth processes on surfaces (i) the LSW theory of Ostwald ripening [4] and (ii) the coalescence of larger clusters [6, 15] will be considered. The distributions resulting from either process exhibit self-similar behaviour, i.e., the distribution at one time can be related to the distribution at later (or earlier) time by a simple scaling factor. If one of these late stage processes are an adequate description of hummock growth then the statistical self-similarity will greatly simplify the description of the process as a function of time. Coalescence is the more natural comparison for the current experimental conditions as it applies to non-mass conserved processes.

In this paper, we examine the properties of hummock formation and evolution on rotating substrates. First, we describe the evolution of a single hummock, followed by binary systems i.e., the coalescence of two hummocks, and then the evolution of a surface covered with hummocks. We then compare these results to the hummocks formed on Ar^+ sputtered Si surfaces. In particular we focus on hummock coalescence and the hummock size distribution and relate this to theoretical models for cluster growth phenomena.

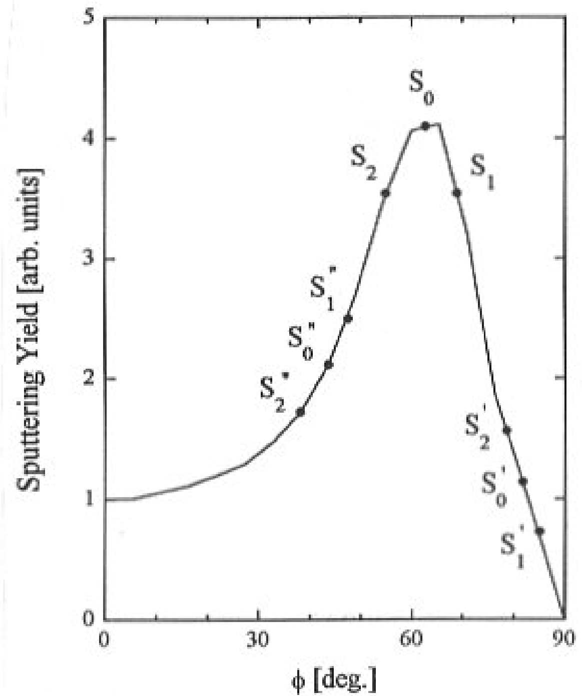

Figure 1. Plot of the sputtering yield, S, as a function of the angle of incidence, ϕ, for Ar^+ sputtered Si [1, 7, 10, 11]. During rotation when, for example, a nominally flat substrate etches at a rate given by S_0, features which deviate several degrees from the flat substrate will oscillate between the endpoints S_1 and S_2 during rotation. However, the features spend the majority of the time at the endpoints. This results in the features etching slower than the flat substrate and macroscopic hummocks form. For a different beam geometry where the flat substrate is etching at S_0', then the features oscillate between the endpoints S_1' and S_2'. For this case the features etch faster than the substrate and no hummocks form (see text). This type of analysis can be carried out for any incident beam direction.

Theory

Evolution of a single hummock

In this section, we derive some results relating to the rate of material loss for features on a rotating substrate. We use a formalism similar to that of Cong-Xin et. al. [5], although our method lends itself well to the description of the evolution of hummock features by simple inspection of the yield curve.

For non-rotating substrates, the rate of material loss is obtained from the S(ϕ) curve in Figure 1. For a rotating substrate, the problem is more complex since the angle between the beam and any features on the substrate is not constant, but changes as the substrate rotates. For the rotating analysis, we use a surface geometry as shown in Figure 2. A nominally flat substrate defines the xy plane and is rotating about the z-axis at an angular velocity ω. Any morphological feature on the substrate is defined by its surface normal, **n**, which subtends

an angle θ with respect to the substrate normal. We refer to θ as the feature angle. The direction of the ion beam, **B**, is defined by the angle ϕ with respect to the substrate normal. The unit vectors describing **B** and **n**, are

$$\hat{B} = \sin\phi\ \hat{x} + \cos\phi\ \hat{z} \tag{1}$$

$$\hat{n} = \sin\theta\cos\omega t\ \hat{x} + \sin\theta\sin\omega t\ \hat{y} + \cos\theta\ \hat{z} \tag{2}$$

With these definitions, the beam direction is defined in the xz plane and the feature normal is in the same plane as the beam at time $\omega t = m\pi$, where m is an integer or zero. The angle between the beam and the surface feature normal, α, is obtained by taking the dot product of Equation 1 and Equation 2 which gives

$$\cos\alpha = \sin\theta\sin\phi\cos\omega t + \cos\theta\cos\phi \tag{3}$$

So that the angle α is not a constant, but α=α(t). The minimum value of α, $\alpha_{min} = |\theta - \phi|$, occurs when ωt is an even multiple of π and the maximum value of α, $\alpha_{max} = (\theta+\phi)$, occurs when ωt is an odd multiple of π.

To calculate the total loss of material per unit area per revolution of the substrate for a particular surface feature, ΔN, we must evaluate

$$\Delta N = 2\sum_{\alpha_{min}}^{\alpha_{max}} \cos\alpha\ S(\alpha)\Delta t(\alpha) \tag{4}$$

where Δt(α) is the amount of time spent in the angular range [α,α+Δα], cosα is proportional to the beam intensity and S(α) is the rate of removal of material for a given α from Figure 1. To evaluate this expression we need the function Δt(α). Using uniform intervals Δα we relate Δα and Δt by the Taylor series expansion

$$\Delta\alpha = \frac{d\alpha}{dt}\Delta t + \frac{1}{2}\frac{d^2\alpha}{dt^2}(\Delta t)^2 + \ldots \tag{5}$$

where Δt=Δt(α). If we take Eq. 5 to first order only, then

$$\Delta t(\alpha) = \frac{\Delta\alpha}{|d\alpha/dt|} \tag{6}$$

This formula is not sufficient, as calculating dα/dt from Equation 3 results in $\Delta t(\alpha) \to \infty$ at ωt=mπ, i.e. singularities results at $\alpha=\alpha_{min}$ when m is even and $\alpha=\alpha_{max}$ when m is odd. To eliminate the occurrence of the singularity in Δt(α) at these points, we must take Eq. 5 to second order. Going to second order gives a quadratic equation which has no singularities and can be solved at all points. In particular, at ωt=mπ,

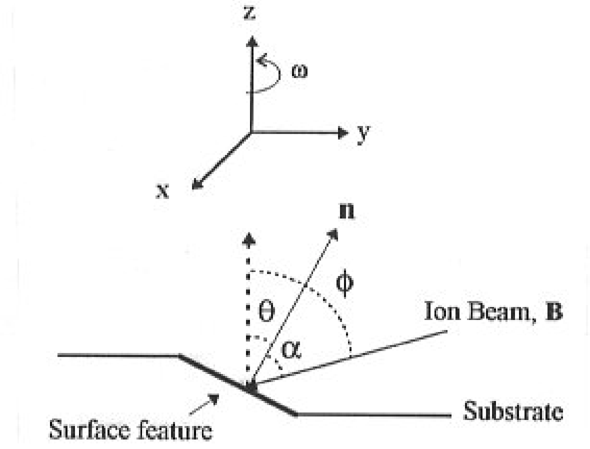

Figure 2. Schematic diagram displaying the geometry during the sputtering process. The ion beam is defined by the angle ϕ and the surface features are defined by θ, with respect to the surface normal. The angle between the ion beam and the feature normal is α. The flat surface is defined by the xy plane and the substrate rotates around the z-axis at an angular velocity ω.

$$\Delta t(\alpha_{min}) = \frac{(2\Delta\alpha)^{1/2}}{\omega}\sqrt{|\cot\theta - \cot\phi|} \quad \ldots m = 0,2,4,\ldots \tag{7}$$

and

$$\Delta t(\alpha_{max}) = \frac{(2\Delta\alpha)^{1/2}}{\omega}\sqrt{\cot\theta + \cot\phi} \quad \ldots m = 1,3,5,\ldots \tag{8}$$

Figures 3a, b and c show plots of Δt as a function of ωt (going to second order in Eq. 5) for the case where ϕ=65° and θ=20°, 40°, and 60°, respectively. From these plots it is immediately apparent that Δt is a sharply peaked function at ωt=mπ so that effectively all the etching of a particular feature occurs at these points (this type of behaviour is analogous to an oscillating simple pendulum, i.e., the amount of time the pendulum spends near the maximum amplitude is relatively large as a result of the small angular velocity, while the pendulum spends a relatively small fraction of the time in the vicinity of the equilibrium position as a result of the large angular velocity). The relative heights of the peaks for m odd versus m even, for a given ϕ and θ, are given by the ratio of Equation 8 to Equation 7. Note that more time is spent at the points where $\alpha=\alpha_{max}$. This effect is, however, outweighed by the fact that the effective area as seen by the ion beam is very large for large values of α, i.e., the beam intensity per unit area

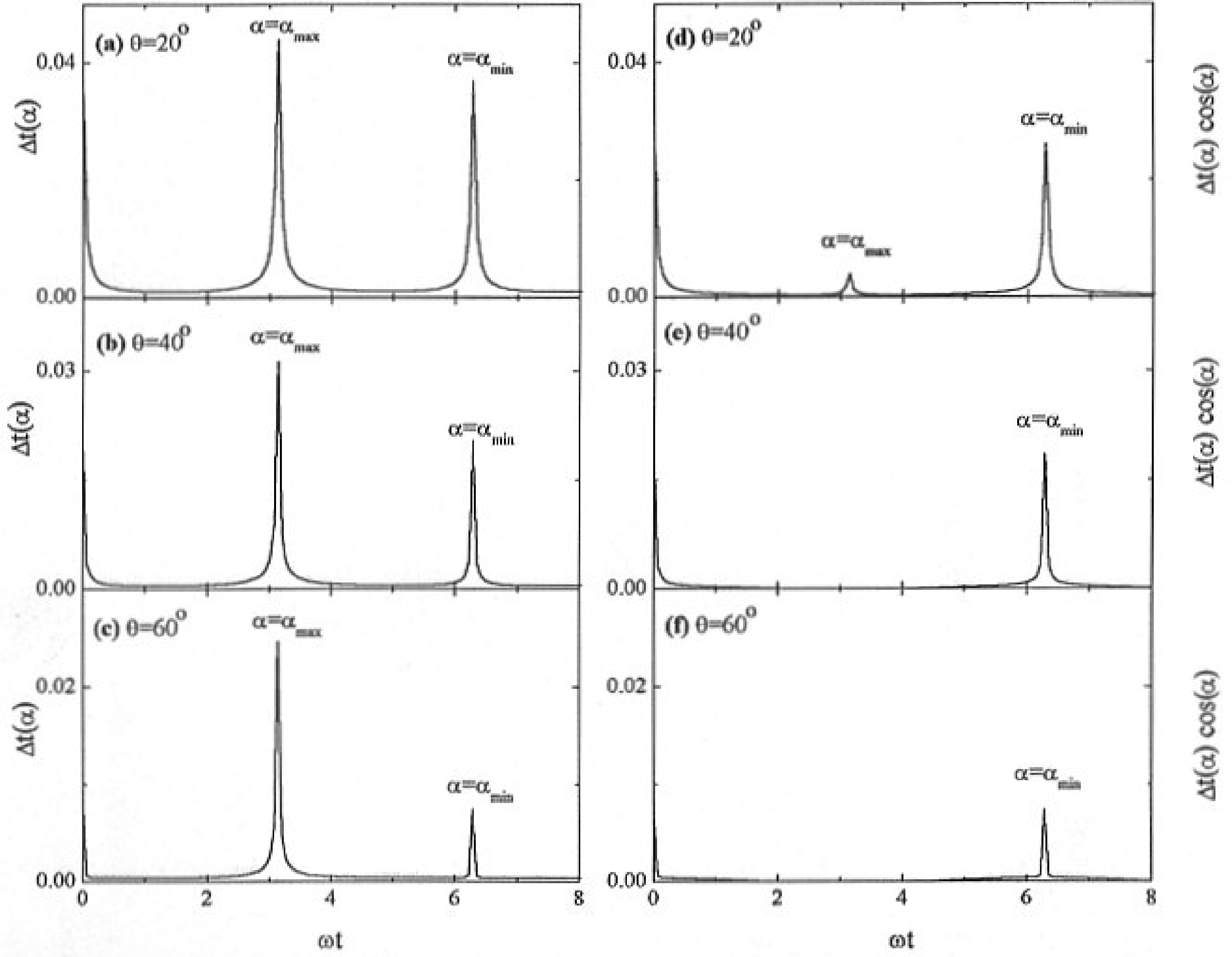

Figure 3. Plots (**a**), (**b**) and (**c**) show the amount of time a surface feature spends in a particular angular range during rotation for θ=20°, 40°, and 60°, respectively. The ion beam angle ϕ=65°. The plots are sharply peaked at α_{min} and α_{max} (see text) indicating that most of the time is spent in these angular ranges during rotation and, as a result, effectively all of the etching occurs for these angles. Plots (**d**), (**e**) and (**f**) are the same as in (a), (b) and (c) except that the time spent in a given angular range is corrected for the beam intensity cos(α).

is greatly reduced. This is evident from Figs. 3d, 3e and 3f which show the function $\Delta t \cdot \cos(\alpha)$ versus ωt for the same cases in Figures 3a, 3b and 3c, i.e., the time spent at each angle corrected by the beam intensity at that time. Note that if $\cos(\alpha)<0$ then no sputtering occurs since the surface feature is shadowed from the ion beam. In general, $\Delta t \cdot \cos(\alpha)$ is largest at $\alpha=\alpha_{min}$ and so most etching occurs at this angle.

With these comments we can now obtain an asymptotic expression for the total loss of material per unit area per revolution, ΔN: we approximate Δt(α) by two delta functions at the points ωt=0,π and so the angular dependent terms can be regarded as constants and taken out of the summation. Thus Equation 4 can be written in the form

$$\Delta N \approx \cos(\theta-\phi)\, S(\theta-\phi) \sum_{\alpha_{min}-w_1}^{\alpha_{min}+w_1} \Delta t(\alpha_{min})$$

$$+\ \cos(\theta+\phi)\, S(\theta+\phi) \sum_{\alpha_{max}-w_2}^{\alpha_{max}+w_2} \Delta t(\alpha_{max}) \qquad (9)$$

where w_i is the "width" of the peak i. We note that w is not the same for both peaks. If we define $2w_i$ as the full width at half maximum of peak i, then we can calculate the width from Equation 5. It is easily shown that, using Equation 5 to second order, the width of the peaks are proportional to the peak height. Specifically, $2w=\omega\Delta t(\omega t=m\pi)$. Then the sums in Equation 9 are proportional to the square of the respective

peak height. Therefore, the total loss of material per unit area for an arbitrary θ and ϕ per revolution is approximated by

$$\Delta N(\theta,\phi) \approx C\cos(\theta-\phi)\left|\cot\theta-\cot\phi\right|S(\theta-\phi)$$

$$+C\cos(\theta+\phi)(\cot\theta+\cot\phi)S(\theta+\phi) \quad (10)$$

where $C \approx 2\Delta\alpha/\omega$.

The first term in Eq. 10 corresponds to $\omega t=0$ and the second term corresponds to $\omega t=\pi$. These two points have different etching rates which depends on the particular values of θ and ϕ. Therefore, the total etching rate of the surface feature can be approximated by the weighted average of the sputtering at these two "endpoints" (given that the total material loss is still the same, i.e. the area under the curve in Fig. 3(a) is not changed, but merely redistributed within the endpoints with the appropriate weighted average). As we describe below, this allows for a simplified description of hummock formation on rotating substrates by visual inspection of Figure 1.

An interesting case occurs under the conditions (i) $\theta=\phi$ and (ii) $\theta+\phi > 90°$ since both terms in Eq. 10 are then zero (the second term is zero due to shadowing). Therefore, this type of surface feature doesn't etch at all, within the approximations we have used. This result is independent of the form of the yield curve (as long as the curve is sufficiently broad so that it can be taken out of the summation as in Equation 9). Therefore, in the long time limit, this is the feature orientation that will survive and one will end up with facetted hummocks. Once a facetted shape is reached as shown by the solid line in Figure 4, it will be maintained as there are no slower etching planes on the hummock. With further sputtering, the base size of the hummock increases since the flat portion of the substrate etches faster than the sides of the hummock. The height, however, remains constant since the top of the hummock and the substrate have the same orientation. The rate of increase in the diameter of the base is constant and does not depend on the initial size of the hummock, only on the etching rate of the flat substrate. The area of the hummock base grows as t^2. Since the height of the facetted hummock remains constant, the shape of the hummock is not strictly conserved during growth. The ratio of base diameter to the top diameter decreases with etching time and approaches the value of 1 in the long time limit.

A simplified method for the description of hummock formation (or lack of hummock formation) can be employed by using Equation 10 and the yield curve in Figure 1. Note that our description does not include effects such as surface diffusion and re-deposition during sputtering. First consider a "perfectly flat" surface which is bombarded with ions. Regardless of ϕ (as long as it is constant), hummocks will not

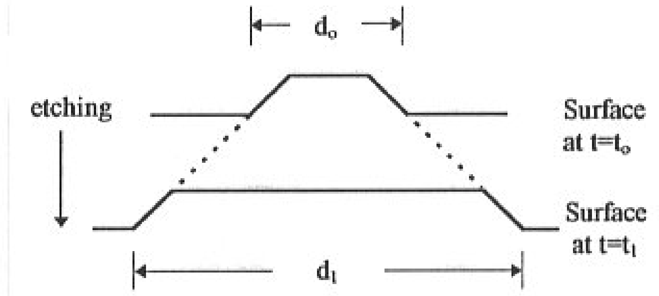

Figure 4. During etching, the base diameter of a facetted hummock increases linearly with time from d_0 to d_1. The height of the hummock remains constant.

form since the entire substrate etches at the same rate. However, if the substrate contains small deviations, e.g., areas with angles of a few degrees off normal, these will, in general, etch at different rates and the evolution of the surface can be inferred graphically from the yield curve. Referring to Figure 1, we assume for example that the angle of the beam with respect to the substrate normal corresponds to the point marked S_0 and the flat substrate etches at this rate. However, a feature angle a few degrees different than the substrate will oscillate along this yield curve, e.g., between the points S_1 and S_2 during rotation. The movement along the yield curve is very fast near S_0 and very slow near both S_1 and S_2, i.e., most time is spent at these two endpoints. With the approximation made in arriving at Eq. 10, the movement is infinitely fast between S_1 and S_2 and all of the time is spent at S_1 and S_2. To determine whether hummocks will form, one must determine if the weighted average of the etching rates at S_1 and S_2 (from Equation 10) is greater than or less than the etching rate of the flat substrate. If this end-point etching is faster than the substrate then the surface features etch faster and no hummocks form. If instead the flat substrate etches faster, then hummocks will tend to form.

Note that deviations from a flat surface are not exclusively required - divergence of the ion beam resulting in deviations in ϕ may also result in similar effects. In addition, defects in the bulk of substrate, which reach the surface after sufficient etching, may etch at different rates and enhance the probability of the nucleation of new hummocks.

We now use this method to illustrate its simple applicability to a few examples with different values of the beam direction ϕ. We assume that the feature angle, θ, with respect to the surface normal is initially no more than a few degrees. The "endpoints" for each value of ϕ are indicated in Fig. 1. In these examples, the time spent at an endpoint is interpreted as $\Delta t\cdot\cos\text{-}(\alpha)$, i.e. the actual time spent at the endpoint corrected for the beam intensity factor.

(a) $\phi \approx 65°$ (S_0, S_1, S_2 case); the average of the endpoints is always less than the etching rate of the flat substrate so the small angle features etch slower, and hummock formation should occur. This is in agreement with the result that hummock formation is most prominent at the maximum of the yield curve.

(b) $\phi \approx 45°$ (S_0'', S_1'', S_2'' case); the average of the etching rates of the two endpoints is about equal to the etching rate of the substrate since this position on the yield curve is approximately an inflection point. However, since relatively more time is spent at the smaller angle where the etching rate is less than the flat substrate, the overall etching rate of the feature is less than the flat substrate and again hummocks form.

(c) $\phi \approx 80°$ (S_0', S_1', S_2' case); this position is also approximately an inflection point of the yield curve and therefore the etching rates at the endpoints is nearly equal to the etching rate of the flat substrate. However, more time is spent in the vicinity of $\alpha = \alpha_{min}$ where the etching rate is significantly higher than the flat substrate. Therefore, the deviations etch faster and the substrate smooths out. Indeed, any value of θ with $\phi = 80°$ gives a similar result. Large θ values will cause shadowing at one endpoint ($\phi > 90°$), but the other, when corrected for the beam intensity will more than make up for any shadowing and the overall etch rate of the feature will be larger than the flat substrate. Sputtering in this geometry is used to avoid hummock formation in SIMS and TEM preparation.

The type of graphical analysis may be carried out at any starting point, S_0, and may also be extended very simply to any system which has an arbitrary yield curve (if one exists that is significantly different than Fig. 1).

Evolution of Two Hummocks

We now turn our attention to the evolution of two hummocks in close proximity on the same surface. As we showed in the previous section, the areal size of a single hummock will increase with time so that if two hummocks exist on the same surface, they will eventually affect each others growth. The interaction of two hummocks is a complicated situation involving partial shadowing of one hummock by regions of the other hummock during rotation. Therefore, we only provide plausible arguments.

We assume that the two hummocks have reached a facetted shape before interaction occurs and that the hummocks are the same height. Also, to simplify the analysis, we assume that interaction does not occur until the bases of the two hummocks are in contact. The evolution of this binary system is depicted in Figure 5, where the coalescence event progresses with time from the top of the figure to the bottom. As sputtering proceeds, the region between the hummocks is shadowed at both its endpoints (Equation 10) so very little etching occurs there and the depression begins to rise relative to the tops of the hummocks. Eventually, the depression region will reach the top of the hummocks an elongated, facetted hummock exists. For simplicity we approximate this as an elliptical shape. Since the growth rate of the base diameter of the hummock, as described in the previous section, applied to one of arbitrary size, both the long and the short sides of the "elliptical" hummock will grow at the same rate. Thus, in the long time limit, the difference between the major and minor axes of the ellipse will remain constant, so the eccentricity of this ellipse will tend to zero and the hummock will approach a circular shape (from a plan view perspective). These arguments suggest that the base shape of hummocks after coalescence asymptotically approaches the shape of a single isolated hummock. The overall shape, however, is not strictly conserved since the height of the hummock remains constant throughout the coalescence event.

If instead the individual hummocks do not have the same base diameter, the description of the coalescence event is similar except in this case the smaller hummock is merely a perturbation on the shape of the larger hummock. The relative size of this perturbation tends to zero as the event proceeds and again a circular shape is asymptotically reached.

Although we have referred to these types of events as "coalescence", it is more appropriately the mutual overtaking of one hummock by another as a result the growth of each individual hummock. Cluster coalescence occurs over a relatively short time scale and is driven by the minimization of surface energies and the equilibrium shape is achieved. This is not the case for hummock coalescence so the process differs from cluster coalescence.

Evolution of a Surface filled with Hummocks

The time-evolution of the hummock size distribution is the most fundamental quantity to describe the global properties of hummock growth. Once the hummocks have reached a facetted shape, the growth of the base of the hummocks is quadratic in time. Superimposed on this quadratic growth is the growth of individual hummocks by coalescence events. Diffusion of material across the surface is typically negligible during hummock formation and growth so it is anticipated that a coalescence-type of size distribution could result. However, deviations from these distributions could occur due to the details of coalescence events (as described above), the lack of shape conservation, and the nucleation rate of new hummocks. If nucleation of hummocks ceases (i.e., since all initial surface imperfections have either formed hummocks or have smoothed-out) then in the long time limit, one hummock will remain on the surface. However, if new hummocks continually nucleate (by mechanisms such as ion beam fluctuations or the etching procedure exposing bulk defects) then the hummock size distribution may approach self-similar behaviour (within the limits of the violation of shape conservation during coalescence events) and comparison to coalescence theories of cluster growth can test these concepts. Note that with facetted hummocks, the appropriate size parameter to plot in the hummock size distribution is the

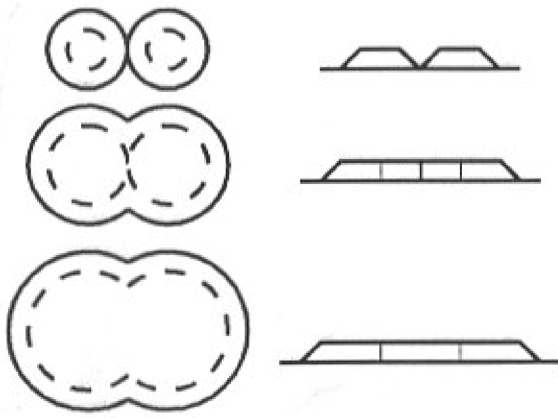

Figure 5. A time sequence showing the coalescence of two hummocks from (**a**) a plan view perspective and (**b**) an edge-on perspective. Time increases from top to bottom. For the plan view, the solid lines represent the base diameter of the hummock and the dashed line represents the flat top diameter of the hummock. The final hummock after coalescence approaches a circular shape and the base shape of the hummock is, therefore, asymptotically conserved after coalescence.

base area of the hummock since the height remains constant. Also, even though the growth of the base of an individual hummock is quadratic in time the global growth rate may not have the same time dependence since coalescence events and nucleation of new hummocks alter the global growth rate from the local one. Testing the quadratic growth rate would require the continual monitoring of the growth rate of isolated hummocks.

Experiment

In this section experimental results of hummock growth on surfaces are presented to test some of the concepts discussed above. As the evolution of individual hummocks has been experimentally well surveyed we concentrate on the coalescence of hummocks and the hummock size distribution. Since the number of parameters that can be varied in the experiments are numerous, and the computing of a hummock size distribution is a lengthy process, we concentrate here on one set of experimental conditions.

Si(100) substrates were cut into 3 mm diameter discs and were mechanically polished with 0.25 µm alumina powder to create a microscopically non-flat surface. This step was done to ensure that hummocks would form under ion bombardment. Cross-sectional TEM analysis of the polished surface reveals a relatively flat surface on a scale of 50 nm and has a dislocation network which extends to about 25 nm below the surface [8]. Ion bombardment on polished samples was done with a commercial E.A. Fischione Ltd. ion milling system at an angle of ϕ=65°. The samples were held at room temperature at a pressure of $1x10^{-4}$ Torr during ion bombardment. Samples were milled with 6 kV Ar^+ ions with beam currents on the order of 200 µA. The rotation of the substrates was approximately 2 revolutions per minute. Scanning Electron Microscope (SEM) images of the bombarded surfaces were obtained with an Hitachi (Tokyo, Japan) S-4500 field emission-SEM.

Figures 6a and 6b show high and low magnification SEM micrographs, respectively, of a sample irradiated for 30 minutes. The individual hummock features are circular and have sizes which range from about 10 µm down to about 1 µm as measured by the diameter of the hummock base. Only hummocks in the central region of a Si disc were analyzed. (The plan view hummock shape near the edge of a Si disc is elliptical rather than circular and is a result of the beam geometry and beam intensity profile, i.e, the gradient in the beam intensity across the surface is not radially symmetric, but is largest perpendicular to the beam direction and smallest parallel to the beam direction). Of particular note in Figure 6 is the large number of coalescence events that are occurring. Some events are just beginning (marked S), others are well under way and appear as figure eight shapes (marked M) and others are near completion (marked E). Two hummocks that have just begun to coalesce each have typically the same shape as an isolated individual hummock and this supports the idea that the shapes of the two individual hummocks evolve, to a reasonable degree, independently until their perimeters begin to overlap. By visual inspection of the events that are at different stages of completion, it is the region between the hummocks that initially “fills in” with material (i.e it etches slower), and eventually the near elliptical shape evolves. As an event nears completion, a circular shape is approached. There are a large number of multiple coalescence events that are occurring, that is, where three or more hummocks are all interconnected and together coalescing (or perhaps more aptly, percolating). In particular is the region P where upwards of ten hummocks are mutually coalescing. A more complete description of the details of coalescence is required, although inevitably this description must also include multiple events since these occur regularly. Also of note in Fig. 6(b) is the tendency for grouping of hummocks in specific regions, while other regions are virtually free of hummocks. This is indicative of non-random spatial nucleation and would depend on the details of the mechanical polishing prior to sputtering.

Figure 7 shows an edge-on view of hummocks. This sample was prepared by milling for only 2 minutes as then the number of coalescence events is reduced and this facilitates the imaging of individual hummocks. The individual hummocks in general have a spherically-capped shape and only a few

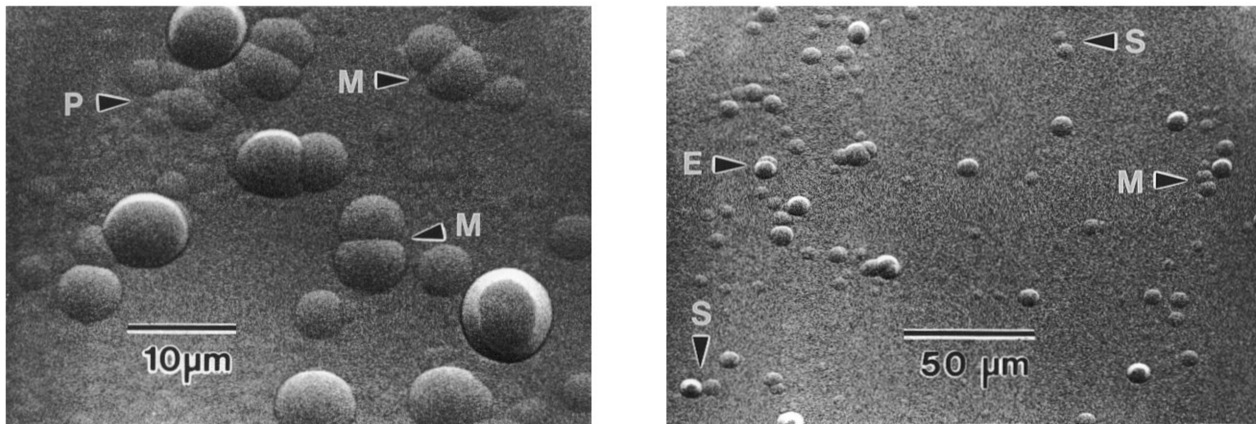

Figure 6. High magnification (**a**) and low magnification (**b**) SEM images of hummocks on Si(100). The beam angle is ϕ=65° and the sputtering time is 30 minutes. The letters indicate different stages of coalescence events: S - start of an event, M - in the middle of an event, E - end of an event, and P - multiple hummocks coalescing.

hummocks have a facetted shape (labelled 'F' in the figure). The contact angle of the hummocks to the substrate is about 25°. The lack of facetted hummocks is due to the short milling time since then selective etching of particular orientations has not had sufficient time to create facetting. Increased milling times tends to increase the number of facetted hummocks, although coalescence events then begin to dominate the hummock shape.

A hummock size distribution was generated from a sample sputtered for 5 minutes. A typical SEM micrograph is shown in Figure 8. The hummock size distribution (HSD) from this sample was generated from many micrographs containing a total of more than 1000 hummocks. We define the size of an individual hummock as the area of its base, A. For cases when two or more hummocks are coalescing, we treat these as one individual hummock with a base area equal to the total base area of the hummocks involved in the coalescence. Since coalescence events were found to typically involve larger hummocks, this approximation method tends not to affect hummocks in the smaller size range. The HSD is shown in Figure 9 where the axes have logarithmic scales. Higher magnification micrographs did not indicate any hummocks at sizes below those plotted. The data fit a power law approximation, $N \propto A^{\mu}$ quite well over the size range of hummocks observed, with μ=-1.6 ± 0.2. Also included in the figure is the theoretical coalescence distribution from Family and Meakin [6] in the asymptotic region of small hummock sizes. This portion of the theoretical curve is (i) the least affected by the assumptions we have made about the size and shape of coalescing hummocks, and (ii) the form the distribution curve initially develops prior to the onset of a bimodal peak at large cluster sizes [6, 15].

The HSD agrees quite well with theoretical distributions over the range of hummock sizes observed. There is however, a discrepancy at small hummock sizes (note again that the data is displayed logarithmically). These deviations from the theory at small sizes can arise from either the details of the coalescence of hummocks or, more likely, the nucleation rate of hummocks during erosion. For the former, theoretical distributions assume that coalescence events occur instantaneously once the perimeters of two individual hummocks touch. This is not the case in our experiments where the time to complete a coalescence event is very long. This allows for multiple coalescence events which may, in part, contribute to the deviations, but this predominantly affects only the larger size hummocks. For the latter, theoretical distributions are based on continuous nucleation of new hummocks and therefore, a reduced nucleation rate in our experiments after sufficient etching would account for the observed discrepancy. This is consistent with other experiments [5] where nucleation is dominated by initial surface imperfections and the rate then decreases once these imperfections have either smoothed-out or nucleated hummocks. In this sense, the time dependence of the deviations in the small size region of the HSD could be used to infer the details of nucleation rates.

Control over the hummock size distribution and the spatial density of hummocks, therefore, requires control over the nucleation rate as etching proceeds. For example, to manufacture HSD's which approach the theoretical coalescence distributions, one needs continuous nucleation of hummocks. Two potential methods for achieving this include: (i) creation of bulk defects that, once they have reached the surface after sufficient etching, act as effective nucleation

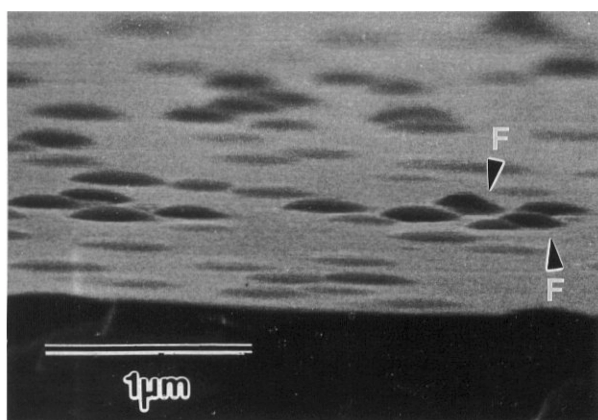

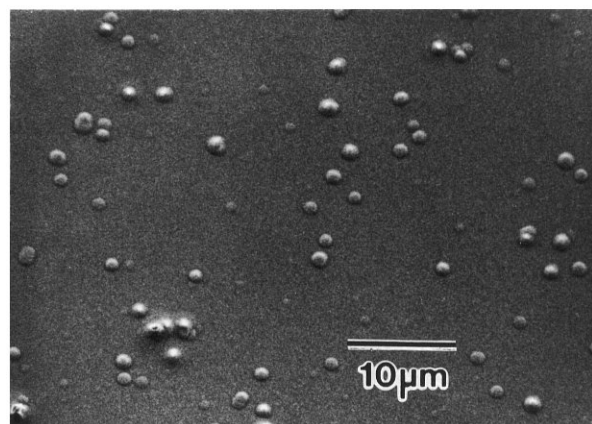

Figures 7 and 8. SEM images of hummocks. **Figure 7** (*at left*). SEM image showing a nearly edge-on view of hummocks formed after 2 minutes of etching at ϕ=65°. Most hummocks have a spherically-capped shape. Some hummocks (marked F) have facetted edges. **Figure 8** (*at right*) SEM image of hummocks formed after 5 minutes of sputtering at ϕ=65°. This micrograph, and others, were used to generate a hummock size distribution.

centres. Such defects could be attainable by Si implantation to generate appropriate defects, or eg., by low dose Co ion implantation which forms small $CoSi_2$ precipitates and this chemical difference may induce hummock nucleation; (ii) sufficient divergence of the ion beam during sputtering. Technically, the second method is preferable if it provides the nucleation rates required. If instead one wants to manufacture hummocks which have a uniform size and uniform spatial density for the potential application of creating patterned surfaces for heteroepitaxial overgrowth, one needs a large nucleation rate for a very short period of time followed by a nearly complete suppression of hummock nucleation. Therefore, uniform ion beams and samples with high initial surface defect densities combined with low bulk defect densities are required.

Further experimental studies of the evolution of the hummock size distribution are required. These include the dependence of the distribution on sputtering time, ion beam energy, ion beam current, ion beam geometry, pre-sputtering surface preparation, and treatment of the bulk of the sample to either enhance or inhibit continual nucleation of hummocks.

Conclusions

A theoretical model of hummock formation on rotating substrates has been developed that details (1) the evolution of a single hummock in terms of oscillations along the sputter-yield curve, (2) the coalescence of two hummocks, and (3) the evolution of a hummock-filled surface in terms of a hummock size distribution.

These theoretical concepts were tested for Ar^+ sputtered Si(100). Hummock coalescence events are consistent with the theoretical description where (i) the interaction of hummocks is negligible until the bases of the two hummocks come into contact, and (ii) the base shape of the hummock is asymptotically conserved after a coalescence event. The experimental hummock size distribution deviates from the theoretical model which applies to cluster growth on surfaces. The deviations are most pronounced for small hummock sizes and indicates that the nucleation rate of hummocks is not constant during ion beam etching.

Acknowledgements

I am grateful to T.D. Lowes for help with ion milling and electron microscopy and M. Zinke-Allmang for helpful discussions and the careful reading of this manuscript. This work was carried out with funding from the Natural Sciences and Engineering Research Council of Canada.

References

[1] Bulle-Lieuwma CWT (1991) Transmission electron microscopy of epitaxial cobaltdisilicide/silicon. Ph.D. Thesis, Philips Research Laboratories, Eindhoven, Netherlands. p. 29.

[2] Carter G (1986) Theory of surface erosion and growth. In: Erosion and growth of solids stimulated by atom and ion beams. Kiriakidis G, Carter G, Witton JL (eds.). NATO ASI Series, Series E No. 112. Martinus Hijhoff Publishers, Boston. p. 70-97.

[3] Carter G, Nobes MJ, Webb RP (1981), A second-order erosion slowness theory of the development of surface

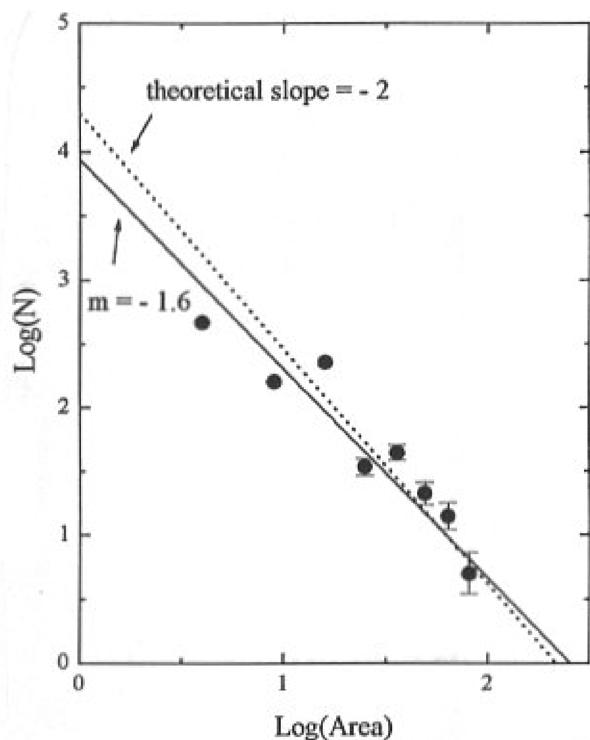

Figure 9. Hummock size distribution (solid circles) from the micrograph in Figure 8 and others obtained from the same surface. The plot is the logarithm of the number of hummocks, N, versus the logarithm of the hummock area, A. The error bars are not shown for small area data points as they are smaller than the points. The solid line is a linear fit to the data with a slope of -1.6 ± 0.2. The dashed line is the theoretical line (slope = -2) for coalescence dominated cluster growth on surfaces [6] in the limit of small cluster sizes.

topography by ion-induced sputtering. J Mater Sci **16**, 2091-2102.

[4] Chakraverty BK (1967) Grain size distribution in thin films - 1. Conservative systems. J Phys Chem Solids **28**, 2401-2412.

[5] Cong-Xin R, Guo-Ming C, Xin-Ding F, Jie Y, Hong-Li F, Shih-Chang T (1983) Topographical changes induced by low energy ion beam sputtering at oblique incidence. Radiation Effects **77**, 177-193.

[6] Family F, Meakin P (1988) Scaling of the droplet-size distribution in vapour-deposited thin films. Phys Rev Lett **61**, 428-431.

[7] Kang ST, Shimizu R, Okutani T (1979) Sputtering of Si with keV Ar^+ ions I. Measurement and Monte Carlo calculations of sputtering yield. Jap J Appl Phys **18**, 1717-1725.

[8] Lowes TD, Zinke-All-mang M (1995) Strained layer epitaxy on rough Si surfaces. Mat Res Soc Symp Proc **379**, 15-20.

[9] Luryi S, Suhir E (1986) New approach to the high quality epitaxial growth of lattice-mismatched materials. Appl Phys Lett **49**, 140-142.

[10] Morgan AE, de Grefte HAM, Warmoltz N, Werner HW, Tolle HJ (1981) The influence of bombardment conditions upon the sputtering and secondary ion yields of silicon. Appl Surf Sci **7**, 372-392.

[11] Sommerfeldt H, Mashkova ES, Molchanov VA (1972) Sputtering of silicon and germanium by middle energy heavy ions. Phys Lett **38A**, 237-238.

[12] Stewart ADG, Thompson MW (1969) Microtopography of surfaces eroded by ion-bombardment. J Mater Sci **4**, 56-60.

[13] Tagg MA, Smith R, Walls JM (1986) Sample rocking and rotation in ion beam etching. J Mater Sci **21**, 123-130.

[14] Tsong IST, Barber DJ (1972) Development of the surface topography on silica glass due to ion-bombardment. J Mater Sci **7**, 687-693.

[15] Zinke-Allmang M, Feldman LC, van Saarloos W (1992) Experimental study of self-similarity in the coalescence growth regime. Phys Rev Lett **68**, 2358-2361.

Discussion with Reviewers

E.A. Fitzgerald: It sounds like defects are needed to form the hillocks, and they are purposefully introduced through the polishing procedure. The defects are not desirable for the heteroepitaxial growth process described, and therefore another method to encourage hillock formation must be used.
Author: Since the defects created by the polishing extend only about 25 nm below the surface, after sufficient ion beam etching the defects would be removed. This appears to be the case for the present experiments since the continual nucleation of new hummocks is reduced as seen by the lack of small hummocks in the size distribution.

As mentioned, the formation of hummocks without the need for surface defects might be realized by a divergent ion beam. This has not been tested.

E.A. Fitzgerald: The strain fields from defects must alter the local sputter-yield curve (Fig. 1) drastically. Therefore, the author needs to develop the theory to employ a spatially variant sputter-yield curve to model this situation.
Author: A spatially variant sputter-yield curve would result in a more complete description of hummock formation and evolution. Particularly with regard to hummock nucleation. However, such an extension of the theory would require, for example, details of the effects of the strain field on the sputter yield and the spatial distribution of the defects that give rise to the strain field. Such a treatment, while needed, is beyond the scope of this paper.

D.D. Perovic: The author mentions a possible technological application of a surface containing hummocks of a uniform size a spatial density for the potential application of creating patterned surfaces for heteroepitaxial overgrowth. Can the author elucidate the mechanism of heteroepitaxial growth on a surface with hummocks.
Author: The mechanism described in the paper by Luryi and Suhir (reference 9) is the geometrical confinement of strain. Specifically, a patterned surface geometry results in the confinement of the strain in the overlayer to the vicinity of the substrate/overlayer interface. If the thickness over which the strain field vanishes is less than the critical thickness for dislocation formation, then the surface of the overlayer would be strain, and defect-free.

D.D. Perovic: The author mentions that the hummocks possess a contact angle of 25°. What is the origin of this specific angle?
Author: Based on Equation 10, the predicted contact angle of the hummock to the substrate for a beam geometry of ϕ=65° is θ=65° since, for this hummock orientation, both terms in Equation 10 are zero and no etching of this feature orientation would occur. The observed value of θ=25° is likely due the slow differential etching between features with θ=25° and features with θ>25°. This can be seen from the yield curve (Figure 1) for the case where ϕ=65° as follows: when θ=25°, one endpoint is at 90° and the other is at 40°. For any larger values of θ, there is no change in the etch rate near the 90° endpoint (the yield is zero for θ>90°) and little change in the etch rate at the other endpoint since the yield curve becomes very flat.